A Study on Structure and Property of Special Sulfonated Petroleum as a Complicated Anionic Surfactant

Fang Yu

Advanced Materials and Analysis Center, National Institute of Clean-and-Low-Carbon Energy, Beijing 102209, China

ABSTRACT

Alkaline/surfactant/polymer (ASP) flooding has been extensively applied to enhancing oil recovery. As an oil displacement agent, pe1troleum sulfonate (PS) is widely used in ASP pilot experiments. It is very important to find a petroleum sulfonate with a high interfacial activity and low adsorption loss. Anionic surfactant petroleum sulfonate is synthesized in a single-tube film sulfonation reactor. PS is separated into fractions with different average molecular weights, and the structure of the fractions is characterized. It has been found out that the interfacial chemistry property of PS is closely related to the molecular structure. The adsorption reaches the maximum value near the critical micellar concentration. Furthermore, there are significantly different interfacial activity and adsorptive property for each fraction. As the lab test result shows, the oil-displacement efficiency for each fraction is changed. The interfacial tension between crude oil and water is declined, and the oil-displacement efficiency of the system is greatly increased as PS or its fraction is used with electrolytes.

Keywords: Petroleum Sulfonate, Interfacial Activity, Molecular Structure, Adsorption, Average Molecular Weight

INTRODUCTION

Oil is a non-renewable energy; after primary exploitation and secondary oil recovery methods are used, 60-70% of the crude oil is still remained in the reservoir. The residual oil needs to be further exploited by means of physical-chemical methods such as enhanced oil recovery (EOR) because of massive requirement for fossil energy. At present, alkaline/surfactant/polymer (ASP) flooding was widely employed for enhancing oil recovery (EOR), which efficiently increased oil recovery by more than 10% compared to water flooding. ASP flooding increased oil displacement efficiency and enlarged the sweep volume simultaneously. The ASP flooding has been developed into the industrial scale and application stage, with a series of important techniques developed in the field tests [1-8].

A low concentration ASP formula is employed to achieve ultra-low interfacial tension with the help of a surfactant. Petroleum sulfonate is a kind of anionic surfactant synthesized by raw

***Corresponding author**
Fang Yu
Email: yufang@nicenergy.com
Tel: +98 86 10 5733 7309
Fax: +98 86 10 5733 7309

Article history
Received: August 14, 2016
Received in revised form: May 14, 2017
Accepted: May 30, 2017
Available online: January 07, 2018

© 2018 Research Institute of Petroleum Industry (RIPI)

material of crude oil or oleum distillates, which is widely applied to ASP pilot experiments. As an oil displacement agent, it owns high interfacial activity, effective compatibility with reservoir fluids, and good water solubility. Furthermore, it is simply produced in the real application situation. Malmberg used nine kinds of petroleum sulfonate samples to perform oil-displacement test and found out that this technology was feasible and had particular advantages [9]. Some patents claimed that petroleum sulfonate was used to discover crude oil efficiently [10-11]. The results of ASP flooding field test in Yumen oil field and Daqing oil field in China showed that oil-recovery was greatly increased when petroleum sulfonate was used [12-13]. There is a good prospect that petroleum sulfonate will be used in enhanced oil recovery. However, the adsorption of surfactant to reservoir rock surface is also an important factor because it reduces oil-displacement efficiency and increases cost. Therefore, it is very important to find the petroleum sulfonate with a high interfacial activity and a low adsorption loss.

The typical property of surfactant mainly depends on the chemical structure [14]. Petroleum sulfonate is a complicated compound containing many anionic surfactants with different molecular structures, which are difficult to be separated into single fractions so as to investigate the interfacial chemical properties [15]. The relationship between the molecular structure and the interfacial property of pure sodium alkylbenzensulfonates have been studied [16-18]. However, the composition of petroleum sulfonate and the relationship between composition and interfacial property have not thoroughly been investigated.

In this paper, a kind of petroleum sulfonate (PS) with an appropriate average molecular weight and a high surface activity was synthesized in a single-tube film sulfonation reactor. PS was separated into fractions with different average molecular weights, and the molecular structure of the fractions was characterized by NMR spectrometry. The interfacial tension (IFT) between PS aqueous solutions and Shengli crude oil, and the adsorption loss of PS on Shengli reservoir sand were determined. The oil-displacement property of PS and its component were also investigated in core-flooding experiments, and the effect of the composition of PS on interfacial properties was discussed.

EXPERIMENTAL PROCEDURES

Chemical Reagents and Materials

PS is synthesized by the raw material of refinery vacuum gas oil (VGO) and SO_3 sulfonation agent. The typical properties of VGO are shown in Table 1.

Table 1: Typical properties of VGO.

Kinematic Viscosity (mm^2/s)		Density (g/cm^3)	Solidification point (°C)	Elemental composition (wt.%)			Chemical composition (wt.%)		
40 °C	100 °C	20 °C	-14	H	C	N	Saturate	Aromatic	Resin
55.40	5.73	0.9383		12.06	87.30	0.24	62.00	37.14	0.86

Sodium hydroxide, ethanol, benzene, isopropanol, chloroform, sec-butyl alcohol, and hydrochloric acid were all analytical reagents. Hyamine 1622, dimidium bromide, and Erioglaucine A were supplied by Fluka Chemical Company.

The crude oil in the experiments was Shengli crude oil obtained from Shengli oil field with an acid

© 2018 Research Institute of Petroleum Industry (RIPI)

number of 1.5 mg KOH/g. Shengli oil field is located in Dongying city, Shandong province in the east of China. The density of the crude oil is 0.9224 g/cm^3 at 30 °C.

The water used in the experiments was the re-injected water of Shengli oil field after filtration. The data of its composition and salinity are tabulated in Table 2.

Table 2: The composition of the re-injected water (mg/L).

K^++Na^+	Ca^{+2}	Mg^{+2}	Cl^-	HCO^{-3}	Total Salinity
4600	106	35	6989	671	12401

The adsorbent in the adsorption experiment is the Shengli reservoir sand from Shengli oil field. The reservoir sand was cleaned with a mixture of methylbenzene/ethanol (weight ratio of 3:1) followed by drying. It was sieved using both 80 and 100 sieve meshes, so its particle diameter was within the range of 0.147-0.175 mm. The composition of reservoir sand was analyzed by X-ray diffraction analysis, it is given in Table 3.

Table 3: The composition of reservoir sand (wt.%).

Quartz	Plagioclase	Potassium feldspar	Clay			
			Kaolinite (K)	Chlorite (Ch)	Illite (I)	Mix-clay (Illite-Montmorillonite)
44	32	22	0.50	0.19	0.32	0.99

In the core flooding experiment, reservoir core (2.5 cm×8 cm) was prepared by using Shengli reservoir sand cemented with epoxide resin and ethylenediamine.

Instruments

PS was synthesized by the single-tube film sulfonation reactor. ^{1}HNMR and ^{13}CNMR spectra were carried out using a Bruker 500-MHz spectrometer. Electrospray ionization mass spectra (ESI-MS, Negative) were obtained using HP1100 MSD. Elemental analyses were performed by an Elementar Vario ELβ. The surface tension was measured by DCAT 21 surface tensionmeter at 20 ℃. The IFT between the PS solutions and crude oil was measured at 80 °C by TX500C interfacial tension meter. The core-flooding experiments were performed utilizing a high-temperature high-pressure core-flooding apparatus.

Synthesis and Purification of PS

PS was synthesized in the single-tube film sulfonation reactor using the raw material of refinery vacuum gas oil (VGO) and the SO_3 sulfonation agent. The sulfonation condition was as follows: sulfonation temperature was 35 °C; the ratio of SO_3 to the aromatic amount of substance was 1.25:1; the concentration of SO_3 was 4.7%, and the mass ratio of the thinner to the raw material was 1.4:1.

PS is the mixture of an active component, an inorganic salt, and the unsulfonated oil. It was purified by a solvent extraction method. The inorganic salt and the unsulfonated oil were separated by solvents such as ethanol, petroleum ether, and n-pentane to obtain the NPS active component. The PS was composed of 78.5 wt.% active component, 8.8 wt.% inorganic salt, and 11.3 wt.% unsulfonated oil.

Separation of PS

With reference to the solvent extraction method

© 2018 Research Institute of Petroleum Industry (RIPI)

determining the equivalent weight distribution of petroleum sulfonate [19], the PS active component was extracted sequentially with different solvents such as benzene, chloroform, and water. A solution of 50 g purified PS (thoroughly deoiled and desalted) in a 750 mL 50 vol.% isopropanol/water mixture was extracted with 700 mL benzene. The benzene layer was removed, and the solvent was evaporated to obtain the benzene extraction part A. The remaining isopropanol/water solution was extracted with 400 mL chloroform to yield chloroform extraction B, and the remaining solution was evaporated to obtain the chloroform residue. The chloroform residue was dissolved in 750 mL sec-butyl alcohol solution saturating with water, and this solution was extracted with 450 mL water to yield water extraction C; the evaporation of the sec-butyl alcohol/water phase yielded the water residue D. The solvents were removed from all the phases, and the residues were thoroughly dried and labeled as fractions A, B, C, and D, which possessed different average molecular weights.

Measurement of Average Molecular Weight of PS and its Fractions

The average molecular weights of the PS and its fractions, namely fractions A, B, C, and D, were measured by the two-phase titration method [20]. The indicator was a mixture solution of dimidium bromide, Erioglaucine A, and H_2SO_4, and the titrating solution was Hyamine1622 solution. The distribution of the average molecular weights of PS and fractions A, B, C, and D were determined by ESI-MS method. Atmospheric pressure ionization electrospray (API-ES) was used as an ionization source, and an 80 vol.% methanol/water solution was regarded as the mobile phase. The flow rate and temperature of the dry gas was 6 L/min and 350 °C respectively, while the nebulizer pressure was 35 psig. The average molecular weights of PS and its fractions were calculated by the following equation:

$$\overline{M} = \sum_{i=a}^{b} M_i \frac{A_i}{\sum_{i=a}^{b} A_i} + 23 \quad (1)$$

where, $\overline{M}$ is the average molecular weight, and M_i is the m/z value; A_i is the abundance.

Characterization of the Molecular Structure of PS and its Fractions

PS and its fractions were reacted with hydrochloric acid to replace Na with H, and petroleum sulfonic acid was obtained. Then, the molecular structure of the petroleum sulfonic acid was respectively characterized by ^{1}HNMR and ^{13}CNMR spectrometry. ^{13}CNMR was obtained with reverse gated decoupling method, and $CDCl_3$ was used as the solvent in NMR measurement

Static Adsorption Measurement of PS and its Fractions

10 grams reservoir sand was mixed with 100 grams PS solution in a ground glass plug Erlenmeyer flask, and it was then shaken for 20 hrs in a water bath at 80 °C. The solution was centrifuged at 3000 rpm for 30 min to separate the reservoir sand. The supernatant was then separated, and the concentration of PS was measured by the two-phase titration. The adsorption amount was calculated according to the concentration change of the PS.

Core-flooding Experiment in Laboratory

The cores were saturated with formation water at a flow rate of 2.0 mL/min at 80 °C to determine pore volume and porosity, and then crude oil was injected until no more water was produced. Then,

© 2018 Research Institute of Petroleum Industry (RIPI)

the formation water was injected until the water content of the produced fluid reached 98%. After water flooding, 1 PV petroleum sulfonate solution was injected to displace the residual oil. At last, the formation water was injected again until the water content of the produced fluid reached 98%. The oil recovery ratio was calculated according to the amount of crude oil displaced.

RESULTS AND DISCUSSION

Molecular Structure of PS and its Fractions

The purified PS was separated into fractions A, B, C, and D which possessed different average molecular weights. The total yield was 99.5%. The average molecular weight of PS and its fractions were measured by two-phase titration method and ESI-MS method simultaneously. The results are given in Table 4. It is clear that the average molecular weight values determined by the two methods are quite close.

The chemical composition and molecular structure of petroleum sulfonate are highly complicated due to the complex composition of the raw materials. Sperling mentioned that it was a compound with a structure changing from $C_{23}H_{38}SO_3H$ to $C_{31}H_{48}SO_3H$, and it was mainly monosulfonate. In this research, the element composition, the ^{1}HNMR, and the ^{13}CNMR spectra of PS and the fractions were measured, and the results are listed in Table 5. Based on the reference method, several important parameters, including average structural parameters of petroleum via NMR spectra, the aromaticity (f_A), and branchiness index (*BI*) were estimated. The average number of hydrogen atoms attached to aromatic carbon ($H_{m)}$ was calculated from the NMR spectra. The f_A value was determined by Brown-Ladner method based on the analysis result of ^{1}HNMR and was double-checked by the number of aromatic carbon and saturated carbon by means of ^{13}CNMR [21]. Then, the range of the average number of carbons(C_T), aromatic carbons(C_A), saturated carbons(C_S), methyls (C_M), and sulfonic groups (N_{SO_3}) were obtained according to the average molecular weight determined by the two-phase titration method.

Table 4: Mass percent and average molecular weight of PS and the fractions.

Sample	Percent (wt.%)	Average molecular weight	
		Two-phase titration method	ESI-MS
PS	100	437	429
A	15.8	666	632
B	35.8	424	412
C	14.3	507	493
D	33.6	402	394

Table 5: The element composition and ^{1}HNMR, ^{13}CNMR data of PS and its fractions.

Sample	H(wt.%)	C(wt.%)	S(wt.%)	*n*(C)/*n*(H)	*n*(C)/*n*(H) corrected value	H_A	H_α	H_β	H_γ	A_A	A_s
PS	8.22	68.06	8.10	0.69	0.72	0.069	0.167	0.485	0.279	2.00	3.45
A	9.72	75.45	5.15	0.65	0.65	0.050	0.197	0.471	0.282	2.00	5.09
B	8.16	63.73	7.57	0.65	0.66	0.053	0.260	0.433	0.254	2.00	4.80
C	7.56	63.45	9.76	0.70	0.71	0.086	0.295	0.432	0.187	2.00	3.31
D	8.07	65.85	8.09	0.68	0.69	0.064	0.275	0.426	0.235	2.00	3.80

© 2018 Research Institute of Petroleum Industry (RIPI)

In Table 5, H_A stands for hydrogens attached to aromatic ring, and H_α, H_β, and H_γ respectively represent hydrogens attached to aromatic ring carbons in alkyl substitution α, in alkyl substitution β, and in alkyl substitution γ; they correspond to the peak area with chemical shifts around 6.0-9.0, 2.0-4.0, 1.0-2.0, and 0.5-1.0 ppm respectively in the ^{1}HNMR spectrum. A_A and A_s respectively represent aromatic carbons and saturated carbons, which respectively correspond to the peak area with chemical shifts around 110-160 and 0-50 ppm in ^{13}CNMR spectrum. The structural parameters of PS and its fractions are listed in Table 6. It is shown that f_A values determined by ^{1}HNMR and ^{13}CNMR spectra are very close, which shows good consistency. In this research, f_A value determined by ^{13}CNMR spectra was used, while the other parameters were calculated.

Table 6: Average structure parameters of PS and the fractions.

Sample	f_A		*BI*	*H*m	C_T	C_A	C_S	C_M	N_{SO_3}
	^{1}HNMR	^{13}CNMR							
PS	0.356	0.367	0.285	0.26	23.9-25.7	8.8-9.4	15.1-16.3	3.4-3.6	1.05
A	0.270	0.282	0.282	0.27	40.3-43.3	11.3-12.2	28.9-31.1	6.3-6.8	1.01
B	0.284	0.294	0.244	0.27	22.9-24.7	6.7-7.3	16.2-17.4	3.2-3.4	0.94
C	0.358	0.377	0.171	0.32	28.8-31.0	10.9-11.7	18.0-19.4	2.6-2.8	1.26
D	0.321	0.345	0.224	0.27	21.3-23.0	7.4-7.9	14.0-15.0	2.6-2.8	0.96

$$f_A = \frac{n(C)/n(H) - (H_\alpha + H_\beta + H_\gamma)/2}{n(C)/n(H)} \quad (^1\text{HNMR}) \tag{2}$$

$$f_A = \frac{A_A}{A_A + A_S} \quad (^{13}\text{CNMR}) \tag{3}$$

$$BI = \frac{1/3H_\gamma}{1/2(H_\alpha + H_\beta)} \tag{4}$$

$$H_m = \frac{H_A}{n(C)/n(H) \times f_A} \tag{5}$$

$$C_{T(max)} = (M - 103)/13 \quad \text{(Assuming all the carbon atoms to be aromatic carbon.)} \tag{6}$$

$$C_{T(min)} = (M - 103)/14 \quad \text{(Assuming all the carbon atoms to be aliphatic carbon)} \tag{7}$$

© 2018 Research Institute of Petroleum Industry (RIPI)

$$C_A = C_T \times f_A \quad (8)$$

$$C_S = C_T - C_A \quad (9)$$

$$C_M = C_S \times BI / ((1+BI)) \quad (10)$$

$$N_{SO_3} = (M-22) \times (\omega(S)\%) / 32 \quad (11)$$

Surface Tension and CMC Value of PS and its Fractions

The surface tension of PS and the fractions in aqueous solutions were measured, and the critical micellar concentration (CMC) was determined from surface tension-concentration curves (Figure 1). The results are shown in Table 7. The surface tension of fraction C is much higher than that of fractions A, B, and D. In addition, the surface tensions of fractions A, B, and D at are very close low concentrations; the surface tension of fraction A is slightly lower than the surface tensions of the others at high concentrations. As found in Table 7, the CMC value of fraction C is higher compared to the other fractions; thus, the surface activity of fraction C is the lowest among the PS fractions.

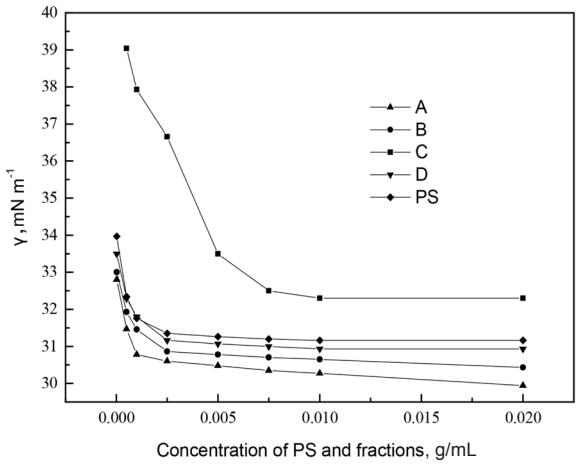

Figure 1: Surface-tension curves of PS and its fractions.

Table 7: CMC and the surface-tension value at the CMC of PS and its fractions.

Sample	CMC ($g.mL^{-1}$)	γ_{CMC} ($mN.m^{-1}$)
PS	0.0025	31.4
A	0.0010	30.8
B	0.0025	30.9
C	0.0075	32.5
D	0.0025	31.2

IFT among PS, the Fraction Solutions, and Crude Oil

Figure 2 shows the IFT among PS; solutions with fractions A, B, C, and D; and crude oil. It was found out that when PS concentration was more than 0.0025 g/mL, the IFT value slightly increased with an increase in concentration. The appearance of the inflection point of IFT curves comes from the formation of a large amount of micelles in surfactant solution, and the concentration at this point is also the critical micellar concentration [14]. Meanwhile, the concentration of petroleum sulfonate monomer reaches the maximum resulting in the lower oil-water IFT. Figure 2 also indicates that the interfacial activity of the fractions shows a significant difference. Among four fractions, the interfacial activity of fraction A is the lowest, while that of fraction C is the highest; the interfacial activities of fractions B and D are quite close. The interfacial activity of the fractions shows the above difference due to their different chemical structures. When surfactant molecules start to form micelles in the solution, and its distribution coefficient between oil and aqueous phase is close to 1, the IFT achieves the minimum value. The interaction between the hydrophobic groups of surfactant molecules induces the formation of micelles. The hydrophobic effect

© 2018 Research Institute of Petroleum Industry (RIPI)

between surfactant molecules is strengthened as the length of hydrophobic chain increases, which enhances the oil-solubility of hydrophobic groups. As a result, surfactant molecules are adsorbed onto oil-water interface more easily, and the CMC of this fraction is reduced. When the number of carbon atoms in hydrocarbon chains of an ionic surfactant is within the range of 8-16, as a homologous compound chain adds one carbon atom, the CMC decreases to half compared with the previous value [14]. Jiang et al. studied the surface properties of sodium polyalkylbenzene sulfonates [17]. They found out that with an increase in the number of carbons in the main chain or the side chains, the degree of CMC reduction is totally different. They reported the influence of the number of carbons of the main chain on the CMC in accordance with the above principles; they also found out that the effect of the side chains in reducing CMC is weaker compared to the main chains. It has been found from Tables 4 and 5 that the more saturated carbon the fraction possesses, the lower the CMC value is, which is satisfied with the above theory. The average number of the saturated carbon of fraction A is much more than that of the other fractions; therefore, the interaction between hydrophobic groups is the strongest, and the oil-solubility is the greatest; the efficiency in reducing IFT is also increased, and CMC value is the lowest. Furthermore, the average number of saturated carbons for fraction A is about fifteen times more than that of fractions B and D, yet the CMC of fraction A is only half of the CMC of fractions B and D, which is perhaps due to the great branchiness index of A. The increase of branched chain enhances the spatial impediment for the petroleum sulfonate molecules to form micelles. Thus, the CMC value of fraction A is slightly lower than that of the other fractions. The average number of the saturated carbons and the branchiness index of fractions B and D are quietly close, and consequently their CMC value is nearly equivalent. The average number of the saturated carbons of fraction C is more than that of fractions B and D, but the CMC value reaches 0.0075 g/mL, which is much higher than the other fractions. Table 4 shows that the number of sulfonic groups of fractions A, B, and D is 1.01, 0.94, and 0.96 respectively, which indicates that they are all monosulfonates. The number of sulfonic groups of fraction C is 1.26, thereby containing a certain percentage of disulfonate. The presence of disulfonate greatly increased the hydrophilicity of petroleum sulfonate molecules and destroyed the original hydrophilic-lipophilic balance. Thus, the average number of the saturated carbon of fraction C is larger compared to the other fractions, while the CMC value is much higher.

The difference in IFT among the PS fractions is also explained by their chemical structures. The structure of the interfacial adsorbed layer, that is the arraying state and the tightness degree of hydrophobic chain present in interfacial adsorbed layer, determines the IFT between surfactant solutions and oil. The difference in the structure of the hydrophobic groups has a significant effect on IFT value, which depends on whether they have an existing branching structure and on the difference in the structure of the end groups. Branching structure can result in a decrease in IFT [14]. Fraction A has a high branchiness index and the greatest average number of methyl. As a result, covering rate (especially CH_3) on oil-water interface is higher, and the array of hydrocarbon chain is much tighter; thus the IFT value is much lower.

© 2018 Research Institute of Petroleum Industry (RIPI)

Among all the fractions, fraction C has the lowest branchiness index. Furthermore, the presence of disulfonate increases the hydrophilicity of molecules, and the ratio of hydrophilic-lipophilic portion is unbalanced; thus, it is very difficult for the molecules to be adsorbed onto interface. As a result, the IFT of fraction C solution is very high.

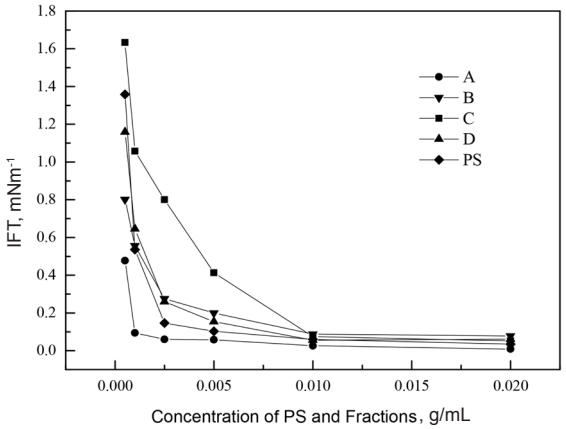

Figure 2: IFT curves of PS and its fractions.

Adsorption Isotherm of PS and the Fractions

Figure 3 shows the adsorption isotherm of PS and the fractions on Shengli reservoir sand at 70 °C. It was found out that within the concentration range of 0.0005-0.0080 g/mL, the adsorption isotherm of fractions A and C is quite similar with that of PS. Their adsorption amount decreased with a further increase in concentration after reaching the maximum value near the concentration of CMC. However, the adsorption amount of fractions B and D decreases after the maximum value, and then rapidly rises. The adsorption isotherm of solid solute was summarized into four types and eighteen varieties [22], and that of fractions B and D belongs to type S, which exhibits the maximum adsorption. The adsorption thermodynamics of anionic surfactant on mineral surfaces have also been studied [23-26]. Liu et al. determined adsorption isotherm of two kinds of sulfonate (ORS-41 and B100) used as oil-displacement agents on oil sand and described their adsorption behavior by the nonuniform surface of two-step adsorption models [23], which showed an adsorption isotherm similar to fractions B and D. Gale separated petroleum sulfonate into three portions with different average molecular weights [27]. They reported that the high average molecular weight component exhibited the strongest interfacial activity and a very big adsorption on clay. It is inferred from Figure 3 that the sequence of the adsorption of the fractions follows the order of water extraction C> water residue D> chloroform extraction B> benzene extraction A. The interfacial activity of fraction A with the highest average molecular weight is the strongest among the four fractions. However, fraction A has the lowest adsorption amount, which is different from the conclusions of Gale. This is due to the difference in composition and structure of sulfonates. Both factors are the intrinsic factors influencing interfacial chemical properties. In the current research, fraction A owns the greatest average molecular weight and the average number of carbons, while Table 4 shows that the average number of aromatic carbons of fraction A is the highest among the fractions, and *H*m value is quite low. *H*m reflects the condensation degree of aromatic rings. The lower the *H*m is, the higher the condensation degree of aromatic rings is. The number of aromatic carbons is great, and the condensation degree of aromatic rings is high. As a result, fraction A contains the most numerous aromatic rings in molecules. Furthermore, its branchiness index is the highest, and the average number of methyls is much greater than that of the others. Thus, there are much more aromatic rings

© 2018 Research Institute of Petroleum Industry (RIPI)

and branched chains in the molecular structure of fraction A. Compared with the other fractions, fraction A contains a greater sectional area, and occupies much larger surface area when it is adsorbed on reservoir sand. Therefore, at the same concentration fraction A has the lowest adsorption amount among the fractions. The number of the aromatic carbon of fraction C is close to that of fraction A, while fraction C has a higher *H*m value, and a lower condensation degree, which enables the number of aromatic carbons of fraction C not to be dominant. Furthermore, fraction C has the lowest branchiness index and the fewest number of methyls. Hence, fraction C does not own the large molecular sectional area. Table 6 shows that disulfonate presents fraction C molecules, in which one hydrocarbon chain is connected to two sulfonic groups, doubling the number of polar groups. When surfactant is adsorbed on a solid surface, the polar groups are adsorbed onto the surface by chemical adsorption or physical adsorption to form the adsorption layer with molecules being in directional arrangement; however, hydrophobic groups stretch into aqueous solution [28]. Thus, the adsorptive capacity of fraction C on a solid surface is stronger, and its adsorption amount is much higher than that of the other fractions.

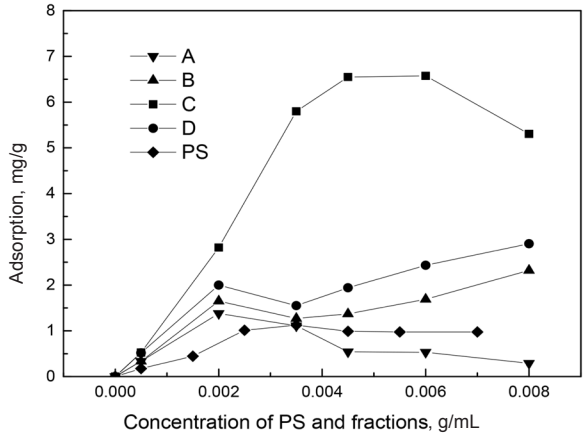

Figure 3: Adsorption isotherm of PS and its fractions.

The Oil Displacement Efficiency of PS and the Fractions in Core Flooding Experiment

The oil-displacement efficiency at a 0.0025 g/mL concentration of PS and the fractions were determined in core-flooding experiments. Furthermore, the different electrolytes such as Na_2CO_3 and Na_2SO_4 were respectively added into PS fraction solutions in order to investigate their effect on the oil-displacement property of PS. The results are shown in Table 8.

Table 8: Oil recovery performance via PS and its fraction with/without electrolytes.

Flooding Solutions	Increasing Oil Recovery (%)		Final Oil Recovery (%)
	Water flooding	Chemical Flooding	
A	38.1	15.8	53.9
B	42.7	10.8	53.5
C	39.2	6.2	45.4
D	39.7	11.2	50.9
PS	38.1	13.9	52.0
A+Na_2CO_3	39.3	31.1	70.4
B+Na_2CO_3	39.6	24.6	64.2
C+Na_2CO_3	38.9	19.9	58.8
D+Na_2CO_3	40.2	25.3	65.5
PS+Na_2CO_3	38.5	28.7	67.2
A+Na_2SO_4	39.7	20.8	60.5
B+Na_2SO_4	39.4	15.2	54.6
C+Na_2SO_4	40.8	10.9	51.7
D+Na_2SO_4	41.1	16.0	57.1
PS+Na_2SO_4	41.5	18.9	60.4

© 2018 Research Institute of Petroleum Industry (RIPI)

It is obvious from Table 8 that the oil recovery is enhanced to the maximum when fraction A is used, while fraction C shows the poorest performance. The oil-displacement efficiency of petroleum sulfonate mainly depends on the interfacial activity and adsorption property, and a surfactant system with the lower oil-water IFT and adsorption loss owns higher displacement efficiency. From the above research, it is concluded that fraction A has the lowest IFT value and the adsorption amount on the sand among all the fractions studied here; thus, it has the maximum oil recovery value. However, fraction C has the lowest interfacial activity and the highest adsorption amount; thus, it has the lowest oil-displacement efficiency. Furthermore, Table 8 shows that when the electrolytes are added to PS solution, the oil recovery increases, and the effect of alkali electrolyte such as Na_2CO_3 is more significant than the others. The reason for the change is that alkali reacts with organic acids in the oil phase to produce surface-active species, which exhibit synergism with PS; this results in a significant increase in the oil recovery value.

CONCLUSIONS

The main conclusions drawn based on the current study are as follows:

(1) PS was separated into four fractions with different average molecular weights. The fractions have a significant difference in their chemical structure. Benzene extraction A contains much more aromatic rings and branched chains. Water extraction C contains a certain percentage of disulfonate, while chloroform extraction B and water residue D exhibit a similar molecular structure.

(2) The PS fractions show a major difference in interfacial activity and adsorption property. Fraction A has a low IFT and CMC value, and it has the largest interfacial activity but the lowest adsorption amount on reservoir sand. Fraction C exhibits the lowest interfacial activity and the highest adsorption loss. The interfacial activity and adsorption amount of fractions B and D are quite close, and they lie between the values of fractions A and C.

(3) Among all the fractions, fraction A has the highest oil-displacement efficiency, and fraction C shows the lowest performance. The oil recovery is obviously enhanced with the addition of electrolytes such as Na_2CO_3 and Na_2SO_4 to PS solution because these electrolytes accelerate the formation of surface-active species in crude oil and increase the concentration of active species on interface. The alkali electrolyte such as Na_2CO_3 has a very significant effect on increasing oil-displacement efficiency.

NOMENCLATURES

BI	: Branchiness index
C_A	: Average number of aromatic carbons
C_M	: Average number of methyls
C_S	: Average number of saturated carbons
C_T	: Average number of carbons
f_A	: Aromaticity
Hm	: Average number of hydrogen atoms attached to aromatic carbon
N_{SO_3}	: Average number of sulfonic groups

ACKNOWLEDGMENTS

The author would like to thank Professor Weiyu Fan for his grateful guidance and help during the preparation of this paper.

© 2018 Research Institute of Petroleum Industry (RIPI)

REFERENCES

1. Rai K., Johns R. T., and Lake L. W., "Oil-recovery Predictions for Surfactant Polymer Flooding," SPE-124001, **2009**, 1-12.
2. Wyatt K., Pitts M. J., and Surkalo H., "Mature Waterfloods Renew Oil Production by Alkaline-surfactant-polymer Flooding," SPE-78711, **2002**, 1-7.
3. Vargo J., Turner J., and Vergnani B., "Alkaline-surfactant-polymer Flooding of the Cambridge Minnelusa Field," SPE-68285, **2000**, 1-6.
4. Pitts M. J., Dowling P., and Wyatt K., "Alkaline-surfactant-polymer Flood of the Tanner Field," SPE-100004, **2006**, 1-5.
5. Sharma A., Aziz Y. A., and Clayton B., "The Design and Execution of an Alkaline-surfactant-polymer Pilot Test," SPE-154318, **2012**, 423-431.
6. Elraies K. A. and Tan I. M., "Design and Application of a New Acid-alkali Surfactant Flooding Formulation for Malaysian Reservoirs," SPE- 133005, **2010**, 1-6.
7. Wang C. L., Wang B. Y., and Cao X. L., "Application and Design of Alkaline-surfactant-polymer System to Close Well Spacing Pilot Gudong Oil Field," Presented at *SPE Western Regional Meeting*, U.S.A., **1997**, 605-619.
8. Wang D. M., Cheng J. C., and Wu J. Z., "An Alkaline/surfactant/polymer Field Test in a Reservoir With a Long-term 100% Water Cut," presented at *SPE Annual Technical Conference and Exhibition*, U.S.A., **1998**, 305-318..
9. Earl W. M., Carolyn C. G., and David M. F., "Characterization and Oil Recovery Observations on a Series of Synthetic Petroleum Sulfonates," *Society of Petroleum Engineers Journal*, **1982**, *22*, 226-236.
10. Hsieh W. C., "Process for Enhanced Oil Recovery Employing Petroleum Sulfonate Blends," U.S. Patent, 4446036, **1984**.
11. Nuckels N., Byth N. J., and Thompson J. L. "Surfactant Compositions Useful in Enhanced Oil Recovery Process," U. S. Patent, 4532051, **1985**.
12. Wang Y., Qiao Q., and Dong L., "A Low Cost ASP Flooding System for Industrial Extending EOR Test at East Block of District VII in Karamay," *Oilfield Chemistry*, **1999**, *16*, 40-42.
13. Wang J., Luo P. Y., and Zheng Y., "The Performance Properties of ASP and Polymer Flooding Solutions Prepared with Hydrophobically Associating Amphoteric Polymers for EOR in Daqing," *Oilfield Chemistry*, **2000**, *17*, 168-170.
14. Zhao G. X. and Zhu B. Y., "Principles of Surfactant Action (2nd ed.)," China Light Industry Press, [Printed copy], **2003**, 1-764.
15. Chen Y. M., Jiao L. M., and Li Z. P., "Synergism Effect of Polar Fractions in Petroleum Sulfonates," *Acta Petrolei Sinica*., **1999**, *20*, 73-77.
16. Wang L., Gong Q. T., and Wang D. X., "Synthesis and Characterization of Sodium Branched-alkylbenzene Sulfonates," *Petrochemical Technology*, **2004**, *33*, 104-108.
17. Jiang X. M., Zhang L., and An J. Y., "Surface Properties of Sodium Alkylbenzenesulfonates with Additional Side Chains," *Acta Physico-Chimical Sinica*., **2005**, *21*, 1426-1430.
18. Nagashima K. and Blum F. D., "Adsorption and Dynamics of Sodium Alkylbenzenesulfonates on Alumina," *Colloids and Surfaces A: Physicochem. Eng. Aspects*., **2001**, *176*, 17-24.

© 2018 Research Institute of Petroleum Industry (RIPI)

19. Sandvik E. I. and Gale W. W., "Characterization of Petroleum Sulfonates," *Soc. Pet. Eng. J.,* **1977**, *17*, 184-192.
20. Brewer P. I., "The Determination of Oil-soluble Sulfonates by Two-phase Titration," *J. Inst. Pet*., **1972**, *58*, 41-46.
21. Brown J. K. and Ladner W. R., "A Study of Hydrogen Distribution in Coal-like Materials by High-resolution Nuclear Magnetic Resonance Spectroscopy II-A Comparison with Infra-red Measurement and the Conversion to Carbon Structure," *Fuel*, **1960**, *39*, 87-96.
22. Lucassen E. H., "Physical Chemistry of Surfactant Action- Anionic Surfactants (2nd ed.)," [Printed copy], New York and Basel, **1998**, 149-150.
23. Liu K. Y., Zhang W. D., and Zhao Ch. J., "Adsorption Thermodynamics of Surfactants for EOR on Oil Sand," *Journal of Beijing University of Chemical Technology*, **1997**, *24*, 9-13.
24. Ziegler V. M. and Handy L. L., "Effect of Temperature on Surfactant Adsorption in Porous Media," Southern California, *Social Petroleum Engineers Journal*, **1981**, *21*, 218-226.
25. Scamehorn J. F. and Schechter R. S., "Adsorption of Surfactants on Mineral Oxide Surfaces from Aqueous Solutions: I: Isomerically Pure Anionic Surfactants," J. *Colloid. & Inter. Sci*., **1982**, *85*, 463-478.
26. [Su H. Y., Zhang C. G., and Zhu Z. Q., "Adsorption Thermodynamics of Sodium Dodecylbenzene Sulfonate on Minerals," Presented at *the 2nd ISTCEI*., U.S.A., **1994**, 360-362..
27. Gale W. W. and Sandvik E. I., "Tertiary Surfactant Flooding: Petroleum Sulfonate Composition-efficacy Studies," *Soc. Pet. Eng. J*., **1973**, *13*, 191-199.
28. Han D. and Shen P. P., "Principles and Application of Surfactant Oil-displacement (2nd ed.)," **2001**, 80.

© 2018 Research Institute of Petroleum Industry (RIPI)